SUPPLEMENTAL NOTES: CASE REPORTS

Family 1 from UAE

F1-II:1

The male index is the first child born to consanguineous (first cousins) Emirati parents. No family history of dysmorphism, developmental delay or infant deaths. There is a family history of metabolic disease, the paternal uncle is married to the maternal aunt who has a daughter with a protein metabolism related disorder.

The index was born at term via vaginal delivery with a birth weight of 2.3 kg. Immediately after birth he required resuscitation due to respiratory distress and was intubated for 2 weeks. On subsequent chest imaging he was found to have pulmonary hypoplasia. He was edematous (as per mother) however, the edema was improving overtime. The mother refers that the baby was severely hypotonic after birth, however, the tone improved with time and physiotherapy. He was noted to have dysmorphic features. The patient was slowly improving and acquiring milestones. He was weaned from the ventilatory support to CPAP, then HFNC and then Optiflow. From 2022, he is on continuous home ventilation using Airvo, and off support during the day and daytime nap. He was fed through an orogastric tube due to the presence of nasal probes for respiratory support continuously. Later, he had gastrostomy tube feeding.

Developmental history: gross motor- head support at 4 months, rolls over at 5 months but not fully, now full roll over from back to tummy, head off table when prone. He can now pull to sit, sit with support for a few seconds. Fine motor- fixed and followed at 2 months, hands together at 4 months, still doesn't reach for objects and unable to transfer. Speech- recently babbles. Social and Behavior- smiles and laughs, enjoys interaction with parents. No concerns with sleep. Normal hearing and vision. In summary, the index presents congenital hypoplasia and dysplasia of lung with pulmonary hypertension due to lung diseases and hypoxia, dysmorphic features, hypotonia and global developmental delay. He is ventilator dependent.

Echocardiogram was normal. Chromosomal karyotype and chromosomal microarray were requested and were normal (no reports are available for review). US abdomen was done and was normal. Chest CT revealed a small left lung. Chest X-rays: Peribronchial wall thickening noted bilaterally with no focal consolidation or collapse. No pleural effusion, no pneumothorax.

A homozygous variant was identified by exome sequencing (Centogene) in the *FBXO22* gene: c.159_162delGGAG, p.Arg53fs.

Family 2 from UAE

F2-II:3

The first patient is currently a 12-year-old male child born to first cousins Emirati parents. He was born prematurely at 36 weeks gestation via c-section. Pregnancy was complicated by reduced fetal movements, and suspicion of hydrocephalus. Birth growth

parameters include weight 1.8 kg, length 45 cm and OFC 33 cm. Shortly after birth, he was admitted to NICU due to hypotonia and respiratory distress, but he did not require invasive ventilatory support. Neonatal course was complicated by feeding difficulty requiring NG tube feeding for 2 years. He was noted to have hypotonia with dysmorphic features including widely spaced and deep-seated eyes, epicanthic folds, depressed nasal bridge, small ears, prominent forehead and micrognathia. Systemic examination revealed that along with the dysmorphic features, he has saliva drooling, generalized hypotonia, joint laxity, mild scoliosis, wide-spaced gait with knocked knees and pes planus. He had right hip recurrent dislocations requiring surgery. He also has a hand tremor. His current growth parameters are weight 23.9 kg, height 110 cm, both are below 3rd centile for age and gender.

Developmentally, he has global delay in all milestones. He crawled at 8 years of age, he was able to sit without support before 8 years old, he stands and walks a few steps with support, only saying Baba/Mama and not being able to hold objects. No regression in his milestones. He has optic nerve atrophy and wears glasses, with no issue with his hearing. He had 2 episodes of up rolling of eyes with arm stiffness when he was 8 years of age, the episodes were very short in duration less than one minute. He was kept on Depaken for 2 months then stopped. His EEG was normal at that time. Currently, he does not have these episodes anymore. He has breath holding spells with hyperventilation whenever he is upset.

The following laboratory investigations were non-conclusive: chromosome microarray with multiple regions of homozygosity, negative exome sequencing. Magnetic resonance imaging (MRI) of the brain done at 4 years of age showed multiple white matter hyper signals more predominantly involving the periventricular central semiovale white matter of both cerebral hemispheres that is almost symmetrically involving both sides with hypersignal on T2 weighted on FLAIR, hyposignal on T1 weighted. Both lateral ventricles are mildly dilated including the temporal horn. The third ventricle and fourth ventricle are normal. Repeated at 8 years of age and showed tiny, some quite confluent white matter hyper signal intensities, bilaterally in the periventricular areas with some cystic/vacuolization changes extending from the frontal, parietal and occipital distribution of white matter. A mild symmetrical dilatation of the lateral ventricles measuring about 1.6 cm in diameter in its midportion with no peri ventricular transependymal migration of CSF which is suggestive of non-pressurized ventricle system possibly due to early loss of volume bilaterally. Bilateral hyper signal intensities in the white matter distribution of both the cerebral hemispheres with lesions lying within 1 cm of the periventricular surface some getting confluent. However, U fibers are not affected. Some of these lesions can also be seen in the corpus callosum, circle semiovale and pons and cerebellar peduncles. The appearances are suggestive of an extensive leukoencephalopathy. No gross abnormality of the neuronal migration, pachygyria or polymicrogyria or heterotopic gray matter visualized. No abnormal signal seen in the hippocampus.

Both renal and echocardiography were normal. Due to his short stature, bone age was done when he was 8 years and 10 months old, showed advanced bone age at least 12 years and 6 months according to Greulich atlas, with partial fusion of the lunate and triquetral.

Due to non-conclusive exome sequencing, genome sequencing was done (Centogene), and a homozygous variant in *FBXO22* was detected c.159_162delGGAG, p.Arg53fs. Parents are heterozygous carriers.

Family 3 from UAE

F3-II:2

This is the second child born to healthy nonconsanguineous Emirati parents, after an uncomplicated pregnancy without exposures or medications. Family history is negative for congenital abnormalities, birth defects, developmental delay, renal disease. There is a healthy male sibling (1-year-old).

The antenatal scans at 4th month showed IUGR with multiple abnormalities: bilateral mild - moderate cerebral ventriculomegaly, mild microcephaly with sloping forehead, perimembranous VSD with no pericardial effusion, double bubble suggestive of duodenal atresia, kidneys were not visualized with certainty, bladder seen and liquor volume normal, amniotic fluid normal. An amniocentesis was performed, and chromosomal karyotype was normal. The patient was born at 35 weeks by c-section given IUGR and breech presentation. The newborn was resuscitated by PPV for 1 min, then she started to cry spontaneously, HR improved immediately after PPV. She was kept on CPAP and transferred to NICU on NCPAP O2 saturation at 5 minutes was 96 %, at 10 minutes was 99% in NCPAP FIO2 100%. APGAR scores were 5 and 7 at 1 and 5 minutes, respectively. Birth weight was 1.6 kg. She presented facial dysmorphism, retrognathia, and right preauricular skin tag.

During NICU stay, she underwent surgery for duodenal atresia after a gastric perforation. There was duodenal atresia with an annular pancreas. A duodenoduodenostomy was performed. The patient was unwell with renal failure postoperatively and had bile-stained gastric aspirates. She received TPN. Enteral feeds were started one month later. She was given a combination of EBM + Special formula milk that progressed to full enteral feeds. Currently, she is taking full enteral tube feeds, with poor weight gain. Renal ultrasound detected small kidneys in their normal locations. The right kidney measures 2.5 cm in length and the left kidney 2.3 cm in length. Both kidneys subjectively appear echogenic with poor corticomedullary differentiation. A cyst is seen in the mid pole cortex of the left kidney measuring 2 mm in diameter. High creatinine levels were compatible with renal insufficiency.

Brain MRI detected moderate dilatation of the lateral ventricles and cerebral mantle thinning associated with partial absence of the septum pellucidum and thinning of the corpus callosum, suggestive of probably underlying neurogenetic etiology. Small retro-cerebellar hematoma. Normal hearing. Vision: occasional squint but normal fix and follow, normal eye exam with no optic nerve hypoplasia. A CNV of uncertain significance (heterozygous deletion on chromosome 16p12.2 was detected on CMA.

The patient presented urinary tract infections, pneumonia; acute kidney failure, diarrhea; and congestive heart failure, disseminated intravascular coagulation and died at the age of 1-year.

A homozygous variant was identified by genome sequencing (Centogene) in the *FBXO22* gene: c.159_162delGGAG, p.Arg53fs. Parents are heterozygous carriers.

Family 4 from UAE (2 patients)

F4-II:2

The index is a female born to 1st degree consanguineous parents from the United Arab Emirates, with an older healthy female sibling. The pregnancy was complicated. At 12+1 weeks: thick NT 4.8 mm. CVS was done and revealed normal karyotype and CMA. At 18+5 weeks: moderate-to-severe hydrocephalus with dilated third ventricle, and mild pericardial effusion were noticed (see image). At 23+5 weeks: cardiomegaly with pericardial effusion were noticed and ventriculomegaly persisted. At 29+5 weeks: in addition to previous findings, severe IUGR and oligohydramnios were observed. At 33+1 weeks: anhydramnios and IUGR were noticed in addition to previous findings. At 34+2 weeks: abnormal umbilical artery doppler (absent end diastolic flow) was observed indicative of placental dysfunction, and the baby was delivered by emergency C-Section

Birth weight was 1.26 Kg, with active resuscitation needed with intubation/mechanical ventilation, and she stayed for 3 months in the neonatal intensive care unit (NICU). NICU course: she developed chronic respiratory failure and became ventilator dependent, chronic kidney failure (end stage, GFR less than 15 ml/min). Ultrasound of the kidneys done during her NICU stay showed polycystic kidneys. Serum creatinine measured at birth was elevated (2.14 mg/dl, normal 0.3-1 mg/dl) and was 1.6 mg/dl at discharge from NICU. Feeding difficulties so she was fed via NG tube, failure to thrive. At discharge from NICU (age 3 months), she had developmental delay. Echocardiogram done at birth revealed a large patent ductus arteriosus and an atrial septal defect that were closed surgically at the age of 5 months.

Two weeks after discharge from NICU, she started having seizures and vomiting blood, and the patient was readmitted to PICU with the diagnosis of seizures, upper gastrointestinal bleeding, and severe metabolic acidosis. During her hospitalization, she had end stage renal failure and continuous renal replacement therapy (CRRT) was started at the age of 4 months. She presented multiple endocrinologic abnormalities (hypothyroidism, secondary hypoparathyroidism of renal origin, hypoglycemia). Brain MRI at age of 5 months revealed dilated irregular ventricles, right parietal cortical cyst, subependymal nodules, thin and hypoplastic corpus callosum posteriorly, gray matter heterotopia, abnormal basal ganglia. Renal ultrasound at 5 months of age showed diffuse echogenicity of the renal parenchyma with both kidneys showing a combination of small and large cysts. There was no corticomedullary differentiation in both kidneys and no pelvicalyceal dilatation. CRRT was complicated with multiple bacteremia episodes, so she was shifted to peritoneal dialysis for some periods. Baby died at age 1 year in PICU after sustaining a cardiac arrest secondary to end stage kidney disease, anuria, sepsis and respiratory failure.

Chromosomal microarray (SNP array) was normal, multiple AOH reported. Exome sequencing (Centogene) detected a homozygous variant in the *FBXO22* gene. M_147188.2:c.159_162del p.(Arg53Serfs*13), parents were heterozygous carriers.

F4-II:3

The patient is an 18-week fetus (sibling of patient 1472624). Prenatal ultrasound showed severe bilateral ventriculomegaly, bilateral renal agenesis, anhydramnios, and ascites, absent corpus callosum, moderate to severe ventriculomegaly and ascites. At 19+5 weeks, IUFD was confirmed. Medical termination of pregnancy was performed. Fetus delivered weighing 135 g. No external malformations were seen, and postmortem study was not performed. Exome sequencing was requested from a prenatal care provider. The same homozygous variant in the *FBXO22* gene NM_147188.2:c.159_162del p.(Arg53Serfs*13) was identified (Centogene).

Family 5 from Oman

F5-II:1

The index is a female born at 32 weeks of gestation; she is the first child of distant related Omani cousins, with no relevant family history. Birth weight was 1.4 Kg. She was operated due to duodenal web and intestinal malrotation. She presented recurrent apneas requiring noninvasive respiratory support. She had subtle dysmorphic features, IUGR, microcephaly, and global developmental delay. She also presented hypothyroidism and anemia. At 4 months old weight of 2.7 kg. She had several hospital admissions due to recurrent apneas necessitating full mechanical ventilation.

Exome sequencing in the index (Centogene) identified the homozygous variant in *FBXO22* NM_147188.3: c.159_162del p.(Arg53Serfs*13). Parents were heterozygous carriers.

Family 6 from Oman

F6-II:1

The male index was born at term to Omani consanguineous (first cousins) healthy parents. There is one healthy sibling. The baby APGAR scores was 8/10, weight 2.3 Kg, length 45 cm, HC 30 cm. He was noticed to have poor sucking with hypoglycemia and was admitted to NICU for presumed sepsis and food intolerance.

The following examinations were done ECHO: small ASD. Head CT: no abnormalities. Abdominal US: Small sized abdominal organs related to small body habits, otherwise normal abdominal study. Microarray: The CGH analysis did not show any pathogenic rearrangements in a male profile.

At 18 months, he can turn, sit with support, and doesn't hold objects placed in hand. He had 9 episodes of tonic clonic seizure with cyanosis that lasted for 3 seconds during the febrile illness. No more seizures. He is not gaining weight - 6.1 kg (below the third centile), height 78 cm (at the third centile), HC: 43 cm. He has dysmorphic features: triangular face, high forehead, hypertelorism, depressed nasal bridge, coxa valga).

Exome sequencing in the index (Centogene) identified the homozygous variant in *FBXO22* NM_147188.3: c.159_162del p.(Arg53Serfs*13).

Family 7 from Oman (2 patients)

F7-II:3

The proband was born to second-cousin parents, a healthy 30-year-old mother, and a 34-year old healthy father. The pregnancy was uncomplicated, and prenatal ultrasound at 21 weeks gestational age (GA) showed symmetrical IUGR, clenched hands, and double air bubbles of the stomach. He was born at 38 weeks GA by emergency caesarean section due to polyhydramnios and breech presentation. His growth parameters at birth were head circumference of 31.5 cm (25th centile), birth weight of 1.9 kg (- 3 SD), and birth length of 42 cm (-2 SD). Physical examination showed facial dysmorphism consisted of a prominent forehead, depressed nasal bridge, short nose with anteverted nares, down slanting palpebral fissures, and hypertelorism with an interpupillary distance of 4.8 cm (+3 SD). He did not have hair upsweep and no cleft lip or palate. Limbs examination showed bilateral clenched hands but normal nails and no joints contractures at birth. Neurological examination showed generalized hypotonia and present deep tendon reflexes with no clonus. The gentile examination was normal male and anus was patent but anteriorly placed.

He developed pulmonary hypertension that required sildenafil and high-frequency ventilation. Pulmonary hypertension resolved within two weeks. He was operated on for duodenal atresia in the first week of life. Annular Pancreas was noted; no intestinal malrotation was observed; duodenoduodenostomy was completed.

At the follow up he continued to have significant global developmental delay. With maximum developmental milestones, he achieved corresponding for 2-3 months. He developed joint contractors and gum hypertrophy.

F7-II:1

Family history is significant for a boy sibling (Family pedigree) with similar facial dysmorphic features and severe intellectual disability. At the age of 8 years, his developmental age was 4-6 months. He was also operated on for duodenal atresia during the neonatal period. His physical examination is detailed in Table X. He was noted to have micropenis but normal testis and anus. He developed generalized tonic-clonic seizures at the age of five years, and he started on valproate; the seizures were controlled.

F7-II:1 and F7-II:3

Investigations for both showed normal liver function tests, renal functions tests, and electrolytes and bone profiles. Echocardiography was normal for the eldest sibling but in the proband showed suprasystemic pulmonary hypertension and small ASD, which both resolved. Screen for inborn errors of metabolism was normal including urine organic acids. Abdominal ultrasound showed no renal malformation. MRI brain showed none specific periventricular white matter T2 hyperintensities but no malformations.

Chromosomal microarray was normal. Both parents provided written informed consent for genetic testing of the proband and the sibling and themselves. This study was approved by the Medical Research Ethical Committee of Sultan Qaboos University (SQU

MREC#1362). Genomic DNA of the proband and family members was isolated from peripheral blood. Initially, sequence analysis of MID1 gene was carried out for the affected neonate, which showed no pathogenic variants. Whole exome sequencing analysis was performed for both affected individuals. In brief, DNA was barcoded and enriched for the coding exons of targeted genes using hybrid capture technology (Agilent SureSelect Human All-exons-V6). Prepared DNA libraries were then sequenced using Next-Generation Sequencing (NGS) technology [NovaSeq6000, 150 bp paired-end, at 200X coverage]. The reads were mapped against UCSC GRCh37/hg19 by Burrows-Wheeler Aligner (BWA 0.7.12). Genome Analysis Toolkit (GATK 3.4) was used for variant calling. Variant filtration was applied to keep novel or rare variants (≤ 1%). Publicly available variant databases and an in-house database of 1562 exomes were used to filter out common or benign variants specific to the Omani population. Only coding or splicing variants were considered. The phenotype and mode of inheritance (autosomal recessive) were considered. Variants of high impact or highly damaging missense, a CADD score ≥ 20 and shared between the affected individuals were prioritized. Other OMIM genes that are known to be associated with a similar phenotype were analyzed from the exome data and no pathogenic variants were identified. Homozygosity for a high impact variant of the FBXO22 (c.159_162delGGAG:p.([Arg53Serfs*13]) was identified in both affected. Sanger sequencing, using the primers 5'TGTGAGCTGTGGGAGAGAC'3 and 5'GCCCAACATTTGATGAACGG'3 confirmed heterozygosity in parents. The variant was also absent from public databases and 1562 in-house population-specific exomes.

Family 8 from Oman

F8-II:1

The index is a female born to healthy Omani parents. She was evaluated at 6 years old due to global developmental delay, hypotonia, dysmorphic features, and seizures. Exome sequencing (Centogene) identified a homozygous variant in *FBXO22* NM_147188.3: c.159_162del, p.(Arg53Serfs*13) in the index, parents are heterozygous carriers.

Family 9 from KSA

F9-II:1

The female index is the first child of consanguineous (first cousins) healthy Saudi parents. There was no history of abortion or neonatal deaths in the family. The patient was diagnosed antenatally by ultrasound scan and fetal echo with severe IUGR, oligohydramnios, hypoplastic right heart, hypertrophied RV, small tricuspid valve, small RVOT, pulmonary valve and PA branches and kidney anomalies. The delivery was at full-term (37 weeks) via (non-complicated) vaginal delivery with birth weight 1.6 kg (<3rd percentile); length: 44 cm (<3rd percentile) and HC: 31 cm (<3rd percentile) APGAR score were 5 and 8. After birth, she was admitted to NICU for symmetrical IUGR, hypoplastic right heart, right hypoplastic kidney and left ectopic (pelvic) kidney. She required mechanical ventilation for 6 weeks after birth for RDS.

She was first seen by a geneticist at 2 month of age and found to have dysmorphic facial features (down slanting palpebral fissure, hypertelorism, broad depressed nasal bridge and microretrognathia) as well short, webbed neck. She was hypotonic with normal power moving all limbs symmetrical, no abnormal movement. Musculoskeletal: club foot, joint

hypermobility, short broad fingers and toes, hypoplastic nails, tapered fingers, dry thick skin and wrinkles, with a large back Mongolian spot extended up to the back between the scapulae. Normal female genitalia. Growth parameters were as follows: weight: 2 Kg (<3rd percentile), Height: 47 cm (<3rd percentile), HC: 32 cm (<3rd percentile).

She has several cardiopulmonary arrests (3X) which resulted in hypoxic ischemic post cardiac arrest and seizure disorder (repetitive myoclonic movement) treated with phenobarbital. She had endocarditis once (negative culture). At 6 months, she was critically ill with on and off desaturation and bradycardia, leading to death.

Renal ultrasound: left renal fossa is empty and left kidney could not be visualized, right kidney measures 3.5x1.5cm with increased cortical echogenicity. Repeated ultrasound is consistent with echogenic small right kidney and ectopic pelvic left kidney in the lower abdomen. DMSA: Normally functioning right kidney, ectopic, normally functioning left kidney. Cystogram: right grade II VUR, ectopic left kidney with grade III VUR. Skeletal survey: periosteal reaction along with extremities, likely prostaglandin related (normal initial one). Head ultrasound: unremarkable. Cardiac echo: hypoplastic right ventricle with hypoplastic tricuspid valve, severe apical RV hypertrophy, hypoplasia of outlet part with small pulmonary valve annulus, normal LV size and function, normal mitral valve. Large PDA 3mm with L-R shunt, echogenic mass seen at SVC-RA junction (most likely thrombus).

Ophthalmology exam: clear cornea and lens on both eyes, fundus exam revealed: OD showed clear media, foveal hemorrhage, peripheral faint old hemorrhage, healthy disc. Repeated exam: Fundus shows bilateral normal optic disc and generalized hyperpigmented choroid and slight hyperpigmented foveal reflex (not surrounded by hypopigmentation which is not consistent with cherry red spot).

Gastrointestinal assessment: Upper GIT study revealed severe gastroesophageal reflux (on continuous N feeding).

Chromosomal analysis: normal karyotype.

Genome sequencing (Centogene) was performed for the index and parents, revealing a variant in *FBXO22* c.8_36delCGGTAGGCTGCTGCGGCGAGTGCCGCGGC, p.Pro3fs (index is homozygote and parents are heterozygotes)

Family 10 from KSA

F10:II-7

The index is a female patient born to Saudi parents, at full term after a Cesarean section (due to previous C-section). The parents are from the same tribe. There are three healthy living siblings, with three late pregnancy terminations and one first trimester abortion.

Pregnancy was uneventful with normal fetal movement, no history of maternal fever or infection. At the age of 6 months parents noticed that the child was not gaining milestones, she was not able to roll over or control her head, there was a history of choking with multiple admissions for respiratory infections at the age of 3 months and 6 months. When the patient was 1-year-old could follow and fixate, recognize her parents, was able to roll

over with partial head control, grasp objects but not transfer from hand to hand. At physical examination, she is awake, alert, not in pain or distress, with subtle dysmorphic features. Microcephalic (HC 43 below 5th centile), weight 5.6 kg, pupils reactive bilaterally, no facial asymmetry, moving all limbs against gravity, reflexes +2, hypotonia axial and peripheral, normal female genitalia.

Investigations: metabolic screening is unremarkable. Brain MRI (at age of 1 year) with bilateral periventricular white matter abnormal signal intensity in the centrum semiovale sparing the subcortical white matter in the immediate periventricular deep white matter. The finding suggestive of metabolic disease, for follow-up MRI with MR spectroscopy and metabolic work-up. Exome sequencing (Centogene) identified a homozygous variant in the *FBXO22* gene - NM_147188.2:c.719_722del p.(Val240Alafs*6) (confirmed by Sanger seq).

Family 11 from UAE

F11:II-2

Pregnancy was uncomplicated until around 7 months when polyhydramnios, decreased fetal activity, and IUGR were noted. The mother felt frequent fetal “hick-ups” during pregnancy. She was born at 37 weeks via repeat C-section and due to breech presentation. At birth, the patient was admitted to the NICU for 3 months due to respiratory distress. She was noted to have dysmorphic features – low set ears, abnormal eyebrow shape, micrognathia, microcephaly, and a prominent forehead. She has hip dysplasia. She failed newborn hearing screen and repeat hearing screen confirmed hearing loss. ABR at 7 months showed moderately severe hearing loss for the right ear (click= 70dB nHL) and a mild/borderline normal hearing loss for the left ear (click = 30dB nHL). Hearing aids were recommended but the patient does not wear them. She also had growth failure, dysphagia, laryngomalacia requiring repair. Swallow test showed aspiration and she was put on nasogastric tube feeding. Parents continue to prefer nasogastric tube to gastric tube feeding. Bolus feeding were tried but she would desaturate and was changed to continuous feeding.

Developmentally, she has only rolled which was around 4-6 months. At 11 months, she was babbling and cooing but had no specific words. She knows her parents and has social smiles. She cannot sit unsupported and does not put weight on her legs when held upright (likely due to hip dislocation). At 2 yo, she has not made any developmental progress, had no sign language and only cries when she is hungry. She cannot sit unsupported. SNP microarray revealed maternally inherited 362 kb 5p15.2 Gain as well as ROH.

arr[GRCh37] 5p15.2(13815741_14178459)x3

arr[GRCh37] 6q14.1q15(78752798_90798564)x2 hmz

Singleton exome sequencing (Centogene) was sent revealed a homozygous the c.159_162del(p.Arg535Serfs*13) variant in FBXO22. Parents were later confirmed to be heterozygote carriers1

Family 12 from UAE

F12-II:4

Patient is a 16 m.o. Emirati female, born to first cousin consanguineous parents, who has been diagnosed to have a homozygous pathogenic *FBXO22* variant related syndrome.

Antenatally, ultrasound showed IUGR, polyhydramnios and intestinal obstruction. Patient was born preterm at 33 weeks through normal vaginal delivery and was admitted to the NICU where she needed respiratory support. She was noted to have a small patent ductus arteriosus and had surgery for a history of duodenal atresia and congenital duodenal obstruction due to annular pancreas. She was noted to have dysmorphic features, plagiocephaly and low set ears. She has had a history of GERD and silent aspiration on NG tube feeding. She has bronchomalacia and chronic lung disease. She has been noted to have generalized hypotonia and delayed development. Renal ultrasound revealed mild left renal pelvis dilatation with mild hydronephrosis. She has been below the third percentile in terms of growth and weight. She has hypotonia and significant motor delay and is unable to grasp toys, does not have head control and is unable to turn at 16 months of age.

Genetic testing: 46 XX with normal microarray. Genetic testing through long read sequencing (Oxford Nanopore) identified a homozygous pathogenic variant in the *FBXO22.*

Family 13 from UAE

F13-II:4 and F13-II:1

At 29 weeks of gestation for *F13-II:4*, fetal ultrasound revealed polyhydramnios, fetal growth restriction, rhizomesomelic shortening of all long bones, left sided talipes, and double bubble (duodenal atresia). The baby was born premature at 35 weeks, she had coartaction of the aorta and jejunal atresia. She died at the age of 8 days from respiratory failure. The parents are consanguineous and there is history of another similarly affected baby (*F13-II:1*) deceased at 2 weeks old. *F13-II:1* presented with IUGR, cleft lip/palate, and intestinal obstruction, with no genetic tests done. This case was excluded from the tally as incomplete phenotyping was done and no genetic testing was done. Meanwhile, prenatal exome sequencing in the fetus of *F13-II:4* (Centogene) identified the homozygous variant in *FBXO22* NM_147188.3: c.159_162del p.(Arg53Serfs*13).

Family 14 from Lebanon

F14-II:1

The patient is a 2y 10-month-old boy born with IUGR at 36 weeks gestational age to consanguineous parents. His birth weight was 2.4 kg. He required oxygen for 1 day in the neonatal ICU in Iraq. At age 3 months he had volvulus which required surgery. 1-day post-op he had seizure that recurred every 3 months. He was started on valproic acid (currently 26mg/kg/day), then levetiracetam (currently 40mg/kg/day) was added. He has history of recurrent otitis, with no reported other chronic infections. He also had failure to thrive and short stature. He has global neurodevelopmental delay. He says 3 words only:

mama, baba and aan. He cannot stand or walk. He can sit without support. Rolling over is not fully mastered.

He is receiving physical therapy. His last seizure was 2 months prior to last visit and presented as left upper extremity tonic clonic movement for few seconds. At physical examination he has short stature (71cm) and weight 7.5 kg. He has hypertelorism and low set ears. Generalized hypotonia, DTR+1 all 4 extremities. He is pale, with puffy face, hands and feet, very dry skin. Blood tests showed macrocytic anemia, high TSH, low freeT4, low parathyroid hormone levels, low ionized calcium, slightly elevated SGPT and SGOT, elevated initial CPK. Abdomen ultrasound was normal, echocardiogram showed biventricular hypertrophy, with a borderline LV systolic function. EKG and EEG were normal, as well as Brain MRI. US Neck/Thyroid: the thyroid gland is not visualized, in keeping with thyroid agenesis. Genome sequencing in the index (Centogene) identified the homozygous variant in *FBXO22*, c.663_666delTGTCinsG p.(Val222del), parents are heterozygote carriers.

SUPPLEMENTAL FIGURES AND LEGENDS

Figure S1. In silico analysis of *FBXO22* alleles.

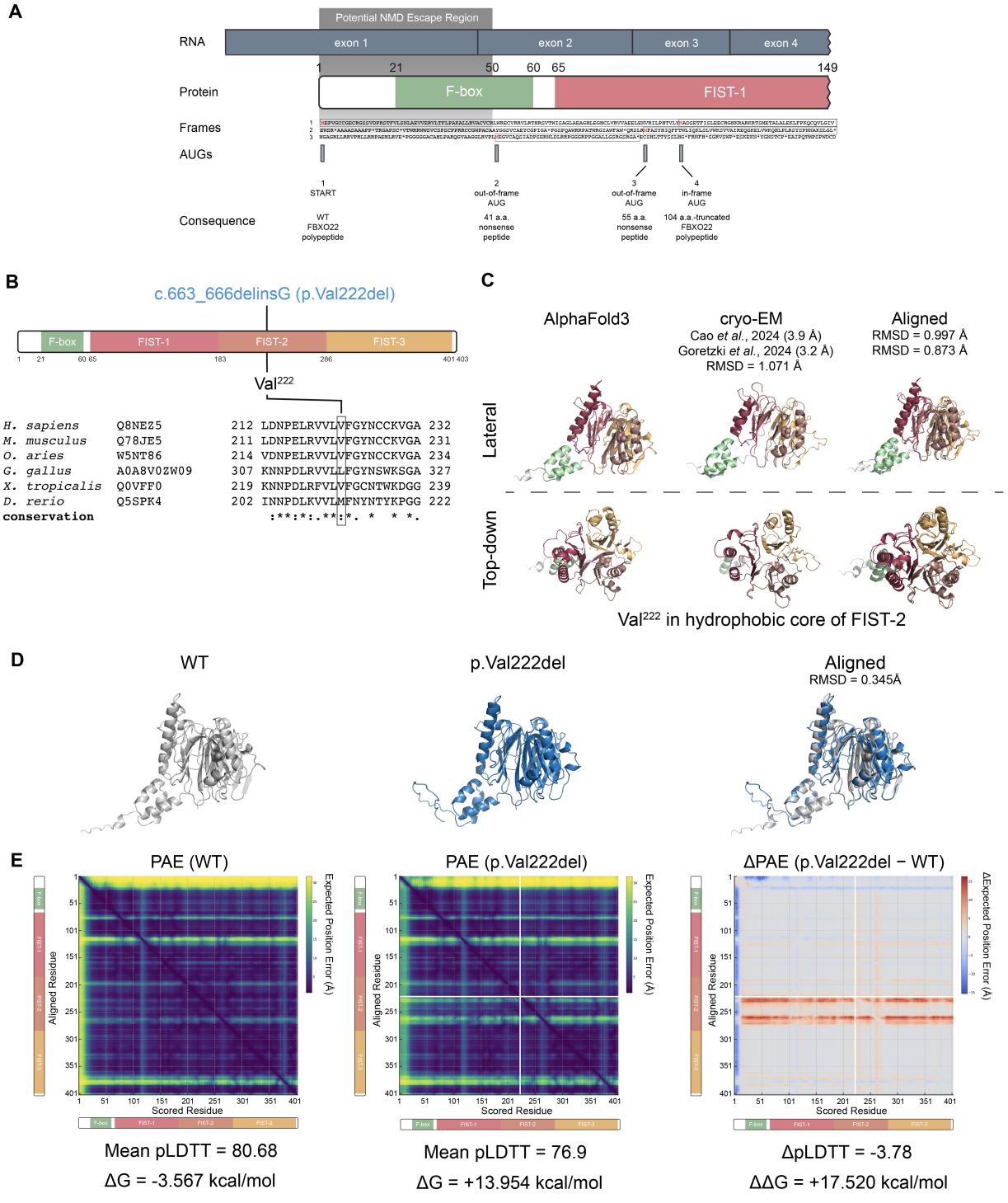

Figure S1. In silico analysis of *FBXO22* alleles. (A) Schematic highlighting the potential Nonsense Mediated Decay (NMD) escape region within the first 150 nt downstream the

start codon of *FBXO22* (grey box) in which the p.(Pro3Leufs*13) variant PTC lies, with the RNA exon structure, protein domain structure and all three frames depicted. All AUGs are indicated, with the peptides made in bounding boxes across the frames, commencing with all theoretical Met residues (labelled in red). (B) Conservation analysis of Val^{222} using Clustal Omega. (C) Lateral and top-down views of the FBXO22 structure model by AlphaFold3 (left), the known Cryo-EM structure (middle) and the aligned AlphaFold3 and PDB:8UA6 structures. Protein domains colored as in panel B. For simplicity of depiction, only the cryo-EM structure from Cao et al., 2024 (PDB:8UA6) is depicted. The resolution of both Cryo-EM structures from Cao et al., 2024 (PDB:8UA6) and Goretzki et al., 2024 (PDB:8S7D) are indicated in brackets (middle), with the RMSD of alignments between the two Cryo-EM structures (middle) and between the respective Cryo-EM structure with the AlphaFold3 model (right) are indicated. Val^{222} is indicated as spheres in all structures. (D) AlphaFold3 models of WT (grey, left), p.Val222del (blue, middle) and aligned structures (right) with the RMSD of alignment indicated. (E) AlphaFold3 Predicted Aligned Error (PAE) scores of every aligned residue (y-axis) against the scored residue (x-axis) of FBXO22 are indicated as heatmaps for WT (left) and p.Val222del (middle) with a false gap inserted for the missing residue for visualization purposes. Differential PAE scores (p.Val222del - WT) are indicated as a heatmap (right). Mean (or differential mean) whole-protein AlphaFold3 predicted local distance difference test (pLDTT) values and free energy of folding (ΔG or $\Delta\Delta G$) calculations of FoldX-repaired WT and variant FBXO22 structures are indicated.

Figure S2. Haplotype and phylogenetic analysis of the recurrent c.159_162del; p.(Arg53Serfs*13) variant.

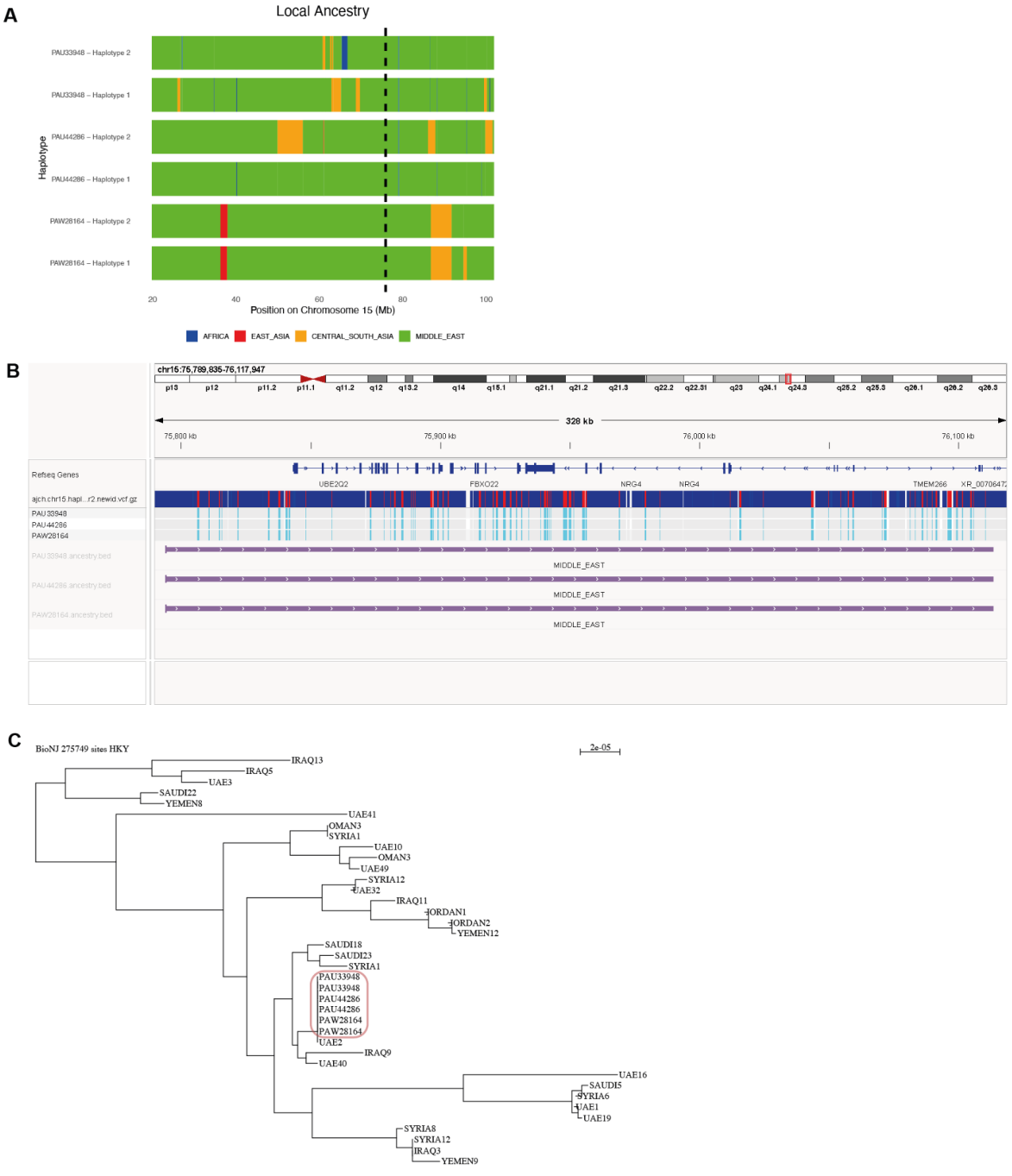

Figure S2. Haplotype and phylogenetic analysis of the recurrent c.159_162del; p.(Arg53Serfs*13) variant. (A) Local ancestry analysis of chromosome 15 for three ONT-seq WGS samples (see Supplementary Methods for details) containing the c.159_162del; p.(Arg53Serfs*13) variant. Dashed vertical line illustrates the location of the variant. (B) hg38 genome browser view of a 328 kb region encompassing the variant identified. Light blue vertical bars indicate homozygous alternative SNPs. All three samples appear to

carry an almost identical homozygous haplotype which is inferred to be of Middle Eastern origin. (C) Phylogeny of the six haplotypes in the three samples alongside 135 published Middle Eastern individuals (see Supplementary Methods for details, a subset of the branch is presented here). The three samples (six haplotypes) investigated in this study cluster together (red box).

Figure S3. Ubiquitous expression of *FBXO22* and *KDM4B*.

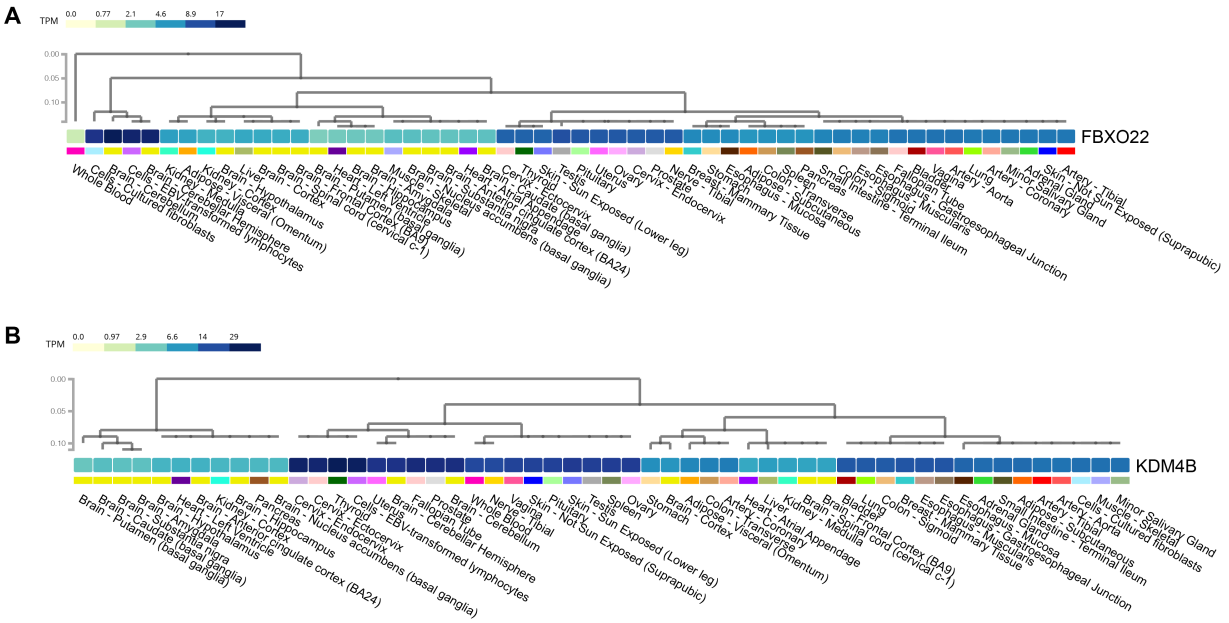

Figure S3. Ubiquitous expression of *FBXO22* and *KDM4B*. GTEx adult expression levels in Transcripts per million (TPM) of (A) *FBXO22* and (B) *KDM4B* indicate that both genes are expressed ubiquitously over different tissue types.

Figure S4. Peripheral blood DNA methylation analysis across known epi-signatures.

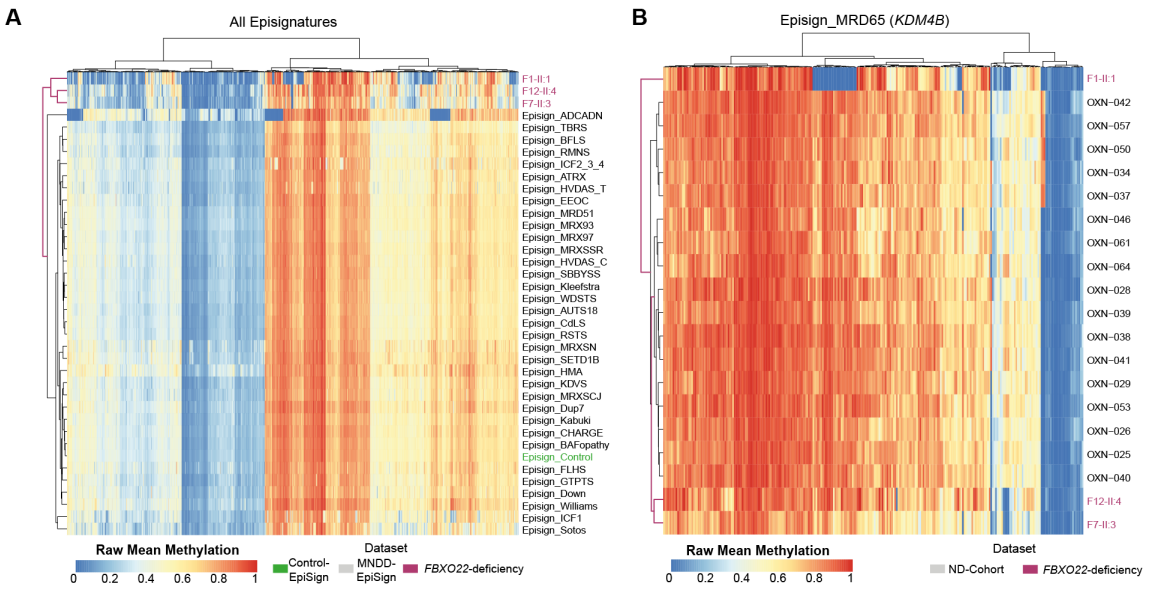

Figure S4. Peripheral blood DNA methylation analysis across known epi-signatures. (A) Heatmap with euclidean distance hierarchical clustering of DNA methylation values for all 3,643 regions featuring known epi-signatures for three *FBXO22*-deficiency peripheral blood samples integrated with the 34 EpiSign Mendelian neurodevelopmental disorders (MNDD-cohort) and EpiSign control dataset. (See Table S4 for EpiSign syndrome acronym definitions). (B) Heatmap with euclidean distance hierarchical clustering of methylation values across 246 regions for *KDM4B* LoF (MRD65)-defining epi-signature regions for the three *FBXO22*-deficiency samples together with an additional dataset of 17 ONT-seq samples with general neurological disorders (ND-cohort).

MATERIALS AND METHODS

Ethical approval

Written informed consent was obtained from all individuals (parents and parents on behalf of patients from each family) for genetic testing, skin biopsy (for patient F7-II:3) and the use of the clinical information and images in this study, according to the ethical approval of the local Institutional Review Boards (IRBs) in U.A.E. and Oman. The study protocol was approved by A*STAR IRB (2019-087) in Singapore and at KAUST (23IBEC090) in the KSA.

Patient recruitment

The affected patient F1-II:1 and F12-II:4 were diagnosed by M.E.B and A.A.T. at Al Jalila Children's Specialty Hospital (U.A.E.). The affected patient F2-II:3 was diagnosed by A.A.Shamsi in U.A.E.. The affected patient F3-II:2 was diagnosed by G.E. in U.A.E.. The affected patient F4-II:2 and fetal case F4-II:3 were diagnosed by H.A., M.A.O. and A.W.E. in U.A.E.. The affected patient F5-II:1 was diagnosed by S.A.S.A. at Armed Forces Hospital, Muscat (Oman). The affected patients F6-II:1 and F8-II:1 were diagnosed by N.A. at the Royal Hospital, Muscat (Oman). The affected patients F7-II:1 and F7-II:3 were diagnosed by A.A. at the Sultan Qaboos University, Muscat (Oman). The affected patient F9-II:1 was diagnosed by M.Alfadhel, F.A. and M.Alghamdi in Riyadh (KSA). The affected patient F10-II:7 was diagnosed by A.A.S. and E.A.F. at the National Neuroscience Institute, Riyadh (KSA). The affected patient F11-II:2 was diagnosed by M.M. in U.A.E. The affected patient F13-II:1 was diagnosed by H.A. in U.A.E.. The affected patient F14-II:4 was diagnosed by H.T., M.A. and S.K. at the American University of Beirut Medical Center (AUBMC), Beirut (Lebanon).

Standard deviation of growth parameters

For individuals with detailed measurements available in Table S1, standard deviation analysis was performed for birth weight, birth length, postnatal (5 years of age and below) weight and postnatal length using the WHO Anthro Survey Analyser software. For head circumference at birth, standard deviation was calculated using the Intergrowth-21st Online Tool. For growth measurements taken from individuals more than five years of age, SD measurement tools were not available.

Next-generation sequencing and analysis

Short-read whole genome sequencing and short-read whole exome sequencing were performed at different research institutes according to local standard procedures:

Exome sequencing. DNA was barcoded and enriched for the coding exons of targeted genes using hybrid capture technology (Agilent SureSelect Human All-exons-V6), as previously described.[1,2] Prepared DNA libraries were then sequenced using Next-Generation Sequencing (NGS) technology [NovaSeq 6000 (Illumina), 150 bp paired-end, at 200X coverage]. The reads were mapped against UCSC GRCh37/hg19 by Burrows-Wheeler Aligner (BWA 0.7.12).

Illumina-short-read-WGS. Short-read whole genome sequencing (srWGS) was done as previously described for F2, F3, F9 and F14.[1] Briefly, using gDNA extracted from whole blood, sequencing libraries were constructed on site using the TruSeqDNA PCR-Free Library Prep kit (Illumina) according to the manufacturer's instructions. Paired-end sequencing was performed on the NovaSeq 6000 platform with the S1 flowcell (Illumina). The reads were mapped against UCSC GRCh37/hg19 by Burrows-Wheeler Aligner (BWA 0.7.12).

Variant analysis. Genome Analysis Toolkit (GATK 3.4) was used for variant calling. Variant filtration, as previously described,[2,3] was applied to keep novel or rare variants (≤ 1%). Publicly available variant databases and an in-house database of 1562 exomes (for the Omani population cases) were used to filter out common or benign variants. Only coding or splicing variants were considered, with splicing variants defined as all variants within a window of +/- 20 bp from the exon-intron boundary. Exomes were analyzed to consider all clinically relevant variants of any inheritance and any diseases, and then candidate genes were analyzed according to priorities, such that the mode of inheritance in this instance (autosomal recessive) was a priority but not the only inheritance analyzed. Variants of high impact or highly damaging missense, a CADD[4] score ≥ 20 and shared between the affected individuals were prioritized. Other OMIM genes that are known to be associated with a similar phenotype were analyzed from the exome data and no pathogenic variants were identified.

Long read sequencing, methylation calling and mapping

Long read whole genome sequencing (lrWGS), processing and methylation calling was done as previously described.[5] Briefly, genomic DNA was extracted from peripheral whole blood using the QIAsymphony DSP DNA Kit (Qiagen) and QIAsymphony automated nucleic acid extraction instrument, according to the manufacturer's instructions. For all samples, 1,000 to 4,500 ng gDNA was sheared with G-Tubes (Covaris LLC, USA) following the standard 20 kb protocol. The resulting DNA fragments were utilized for library preparation using the Ligation Sequencing Kit V14 (Oxford Nanopore, UK), according to the manufacturer's instructions, and was sequenced on the PromethION P48 device with R10.4.1 flow cell (Oxford Nanopore, UK) as follows: 72 hours with a second library loaded at 24 hours post flow cell nuclease flush for FBXO22_F12:II_4 (N50: 11.39kb; Bases: 94.35 Gb; Approximate coverage: 31x); for the low DNA input sample, FBXO22_F1:II_1, DNA shearing was not performed and the library was sequenced for only 72 hours (N50: 14.9 kb; Bases: 34.5 Gb; Approximate coverage: 11.5x); for FBXO22_F7:II_3 the library was sequenced for 97 hours with second and third libraries loaded post-nuclease flushes at 28 hours and 52 hour timepoints (N50: 11.5 kb; Bases: 110.1 Gb; Approximate coverage: 36.7x). Base calling (with 5mC) was done using "high-accuracy base calling" (HAC) mode during the run using MinKnow distribution (v22.05.7 or v24.02.19) and Guppy/Dorado (v6.1.5 or v7.3.11). The methylation SAM tags (MM,ML) were preserved using samtools (version 1.13) for all BAM passed files and were then aligned to the human reference genome (GRCh37/hg19) using minimap2 (v2.22-r1101) using the appropriate parameters '`minimap2 -x map-ont -a -y`'.

Methylation profile analysis

Methylation analysis was performed by comparing the methylation profile of the affected individuals with those reported in literature for the Episign epigenomic signature[6] for a total of 34 Mendelian neurodevelopment disorders (MNDDs). We also included the Episign control dataset representing the mean of "general population samples with various age and racial backgrounds"[6] to remove confounding effects of age and ethnic differences. For the purpose of comparison, disease specific probes from Illumina Infinium methylation 450k and EPIC bead chip arrays identified as epi-signatures (EpiSign) were mapped on the human genome hg19 using pblat15 with the parameter "`-fastMap`". In order to remove ambiguity coming from multimapping probes, those with block count of 1 with alignment length matching the probe length were selected and assessed for the downstream analysis. Aggregated methylation modification counts for each base from long read sequencing in the probe region were calculated using modbam2bed from the 'methyl' module of Epi2Me workflow wf-human-variation (v1.2.0). Methylation values for all samples and MNDD dataset were standardized (i) and normalized (ii) using min-max normalization using the equation below where s is the sample, p is the probe, x_p is the methylation value for each probe, $\overline{x}$ is the mean and $\boldsymbol{\sigma}$ is the standard deviation, stdMethyl is the standardized methylation value and normMethyl is normalized methylation value:

$$(i) \qquad stdMethyl_p = \frac{\overline{x_s} - x_p}{\sigma_s}$$

$$(ii) \qquad normMethyl_p = \frac{stdMethyl_p - min(stdMethyl_s)}{max(stdMethyl_s) - min(stdMethyl_s)}$$

Hierarchical clustering was performed using euclidean distance and ward.D2 for MNDD epi-signature probes on normalized methylation values for each sample with the MNDD. For the *KDM4B* Episign probe set[7], hierarchical clustering was performed using euclidean distance and ward.D2 on the normalized methylation values for the *FBXO22*-deficiency samples and our additional cohort of previously published ONT-seq reads from 17 unrelated Neurological Diseases (ND-cohort; Middle Eastern).[5] IGV v2.16 was used to visualize differentially methylated regions of interest from the ONT-seq reads.

FBXO22 epi-signature detection and analysis

In order to identify a specific FBXO22 methylation signature, we focused on regions defined by 3,643 probes from the published Episign epigenomic signature dataset[6] for a total of 34 MNDDs. Standardized and normalized methylation values were calculated, as mentioned above. The FBXO22_F1-II:1 sample sequenced with low input DNA protocol was observed to show higher variability within the replicates, suggesting technical variability. Hence, probes with low variability within the replicates were considered. Briefly, probes with high variability within the FBXO22 sample replicates were removed such that the standard deviation of each probe of the replicates were within the 75th quantile, thus negating effects of technical variability within the replicates. Methylation difference was calculated for each probe between the MNDD and FBXO22 (i), where p is the probe, methylDiff is the methylation difference, $\overline{\mathrm{FBXO22}}$ is the mean methylation value of the replicates of FBXO22, and $\overline{\mathrm{MNDD}}$ is the mean methylation value of the 34 MNDDs:

$$(i) \qquad methylDiff_p = \overline{FBXO22_p} - \overline{MNDD_p}$$

The optimal probe set for FBXO22 (40 probes) was selected by an iterative method of probe selection based on the ranked decreasing value of the methylDiff such that the cumulative explained variance for principal components 1 and 2 was at least 60% with least correlation across the MNDD (Supplementary Tables S2 and S3).

Probes were classified as hypermethylated or hypomethylated as below:

$$\mathrm{Log2}_p = \begin{cases} \text{hypomethylated}, & Log_2\left(\dfrac{\overline{FBXO22_p}}{\overline{FBXO22control_p}}\right) < 0 \\ \text{hypermethylated}, & Log_2\left(\dfrac{\overline{FBXO22_p}}{\overline{FBXO22control_p}}\right) \geq 0 \end{cases}$$

Where $\overline{FBXO22_p}$ and $\overline{FBXO22control_p}$ refer to the average methylation values of three FBXO22-deficiency affected individuals and two controls from the ND ONT-seq cohort respectively for the probe *p*. Each differentially methylated probe was analysed for overlap with annotated genes or proximal regulatory elements within 100 kb upstream of genes. Tissue-specific expression profiles of the identified genes were evaluated using GTEx and the Human Protein Atlas, prioritizing those expressed in tissues relevant to the observed phenotype. Functional annotations and disease associations alongside existing literature were reviewed to evaluate whether altered gene expression or differential methylation had been reported in phenotypically overlapping cases. This integrative approach identified 20 differentially methylated regions (Table 2 and S3) as most likely to play a role in the observed syndrome, based on their functional significance, expression in affected tissues, and phenotypic relevance, and ranked in Table 2 from most hypomethylated regions to most hypermethylated compared to the controls.

Haplotype and phylogeny analysis

ONT-seq lrWGS for the three samples were mapped using minimap2[8] (v2.28-r1209) using the preset parameter (`map-ont`) to GRCh38. SNP genotype likelihoods were generated using bcftools (v1.17) using the following command on polymorphic sites found in the HGDP+APPG reference panel:

```
bcftools mpileup -B -Q13 -q30 --max-BQ 30 -I -E -T chr15.reference.panel.vcf.gz -b <bam.list> -Ou | bcftools call -Aim -C alleles -T chr15.reference.panel.sites.tsv.gz -Oz
```

This panel is composed of the 929 HGDP samples[9] and an additional 135 APPG (Middle Eastern) samples.[10] The construction of the panel is described in the supplementary of Martiniano et al., 2024.[11] Beagle4.0[12] was subsequently used to refine genotypes based on genotype likelihoods using the HGDP+APPG reference panel. Only highly confident sites (AR2 > 0.98) were retained for analysis. Beagle5.4[13] was then used to phase variants into haplotypes using the same reference panel. FLARE[14] (version 0.5.1) was used to perform local ancestry inference using the HGDP samples as a reference with seven reference ancestries set as previously described[9]: Africa, Europe, Middle East,

East Asia, Americas, Oceania and Central & South Asia. A phylogeny based on SNPs within the region (chr15:75794242-76113817) was generated based on fasta sequences that were produced for each haplotype using bcftools consensus (v1.17). The distance-based phylogeny (HKY) was built using seaview (v5.0.5)[15]. The three individuals were analysed along with the aforementioned 135 Middle Eastern samples. Due to the large phylogeny, only the branch with the three samples is illustrated.

Cell culture

The affected primary cutaneous fibroblast cell line was established from a skin biopsy from F7-II:3, following standard procedures, with the WT line previously derived.[16,17] All primary fibroblast lines were cultured in complete Dulbecco's Modified Eagle Medium/High Glucose (with 4 mM L-glutamine) (HyClone Cat: SH30022.01) supplemented with 10% fetal bovine serum (FBS) (Biological Industries) and 1% penicillin-streptomycin (Gibco). For treatment with cycloheximide (CHX), 250,000 cells of fibroblasts were seeded per well of a 6-well plate. 24 hours later, 100 ug/ml final concentrations of CHX (Cell Signalling Technology) in DMSO was added to the cells, prior to lysis at 0 and 24 hour timepoints. For overexpression experiments, the following constructs were used: pMAX-copGFP (GFP) from Lonza and pcDNA3.1(+)-N-DYK(FLAG), with HA tag N-terminal to WT *FBXO22* CDS or p.Val222del (Genscript), which was Sanger-sequence verified. 350,000 HEK293T cells were seeded and reverse transfected with 2 ug of plasmid DNA with FugeneHD reagent (Promega) at a 3.5:1 ratio, on 0.01% poly-L-Lysine (Sigma) coated plates. The same media as above was used. 24 hours later, media was replaced. 48 hours post transfection, cell lysates were taken for downstream RNA and protein analysis. All cell lines were maintained in a humidified atmosphere at 5% CO_2 and 37°C and tested negative for mycoplasma using the MycoAlert Mycoplasma Detection Kit (Lonza, catalog no. LT07-118).

RNA extraction and RT-qPCR

Total RNA from cell culture was extracted using the RNeasy Mini Kit (Qiagen) according to the manufacturer's instructions. For RT-qPCR analysis, cDNA was synthesized using a ReverTra Ace qPCR kit (Toyobo). RT-qPCR amplifications were then performed in 96-well optical reaction plates with Power SYBR Green PCR Master Mix (Applied Biosystems) on the QuantStudio 3 System (Applied Biosystems). The relative expression values of each gene were determined by normalization to beta-actin expression for each sample. For the treatment with CHX and experiments with HEK293T cells, total RNA was extracted using the RNeasy Plus Micro Kit (Qiagen) according to the manufacturer's instructions. For RT-qPCR analysis, cDNA was synthesized using iScript (Bio-Rad). RT-qPCR amplifications were then performed in 384-well optical reaction plates with Power SYBR Green PCR Master Mix (Applied Biosystems) on the QuantStudio 7flex System (Applied Biosystems). The relative expression values of each gene were determined by normalization to both GAPDH and beta-Actin expression for each sample. For all experiments, different passage numbers on different days were used for each replicate (n = 3) per cell line, with three technical replicates additionally performed per replicate for qPCR measurement. Prism v10 was used for statistical analysis of RT-qPCR data.

Cell lysate and western blotting

Cells were directly lysed with Laemmli-buffer (2% SDS, 10% glycerol, 5% 2-mercaptoethanol, 0.002% bromophenol blue, and 62.5 mM Tris HCl at pH 6.8). Whole lysates (20-50 g) were separated by SDS-PAGE, transferred to a PVDF (Immobilon-P; Millipore) membrane, and then subjected to immunoblotting with the appropriate antibodies using the ECL detection system. For HEK293T experiments, cells were trypsinsed with 2.5% trypsin (Gibco), pelleted and snap frozen. Pellets were lysed with Pierce RIPA buffer (ThermoFisher Scientific) and 1x Pierce EDTA-free protease inhibitors (ThermoFisher Scientific). 30ug clarified lysates were boiled with Laemmli-buffer and separated with SDS-PAGE, and transferred to PVDF membranes (Bio-rad, 1704156). The iBright1500 system (ThermoFisher Scientific) was used for ECL detection. FIJI was used for quantification of western blot signals using the Gel tool. Prism v10 was used for statistical analysis of quantified western blot data. Different passage numbers (with independent transfections) on different days were used for each replicate (n = 3) per cell line.

In silico protein analysis

Protein sequence conservation analysis of FBXO22 was performed with the Clustal Omega program (v1.2.4) on UniProt. For modelling the single amino acid deletion variant p.Val222del, a modified strategy was followed[18]. Top confident AlphaFold3[19] structures were used to model FBXO22 WT (Q8NEZ5) and p.Val222del structures, with AlphaFold3 pLDTT and PAE values subsequently analysed and visualized with in-house python and Matplotlib code (https://doi.org/10.5281/zenodo.15022895). PyMOL (v3.0.3) was used for all protein visualization, alignment of models (including cryo-EM structures PDB:8UA6 and PDB:8S7D) and RMSD calculations. For free energy calculations, FoldX (v5.1) RepairPDB parameter was used to minimize free energy calculations by optimizing side chains and removing clashes. The Stability parameter was then used for free energy calculations.

List of antibodies used

mouse anti-ACTB (AC-15: Santa Cruz Biotechnology)
rabbit anti-FBXO22 (GeneTex, GTX117774)
rabbit anti-KDM4B (Cell Signaling Technology, D7E6)
mouse anti-GAPDH (sc-32233: Santa-Cruz Biotechnology)
mouse anti-FLAG(M2) (Sigma, F3165)

List of primers used

ACTB-forward primer: AGAGCTACGAGCTGCCTGAC
ACTB-reverse primer: AGCACTGTGTTGGCGTACAG
GAPDH-forward primer: CGCTTCGCTCTCTGCTCCTCCTGT
GAPDH-reverse primer: GGTGACCAGGCGCCCAATACGA
FBXO22-forward primer: CTCACTGAAGTAGGTCTTTTAG
FBXO22-reverse primer: CCAGCCAAGATGATATTCATATC
KDM4B-forward primer: TGTCTGATGAGCGTGAAAGG

KDM4B -reverse primer: GTTGGAGGAATCAGCCAAAA
FLAG-HA-FBXO22-forward primer: ACAAGGATGACGACGATAAGGG
FLAG-HA-FBXO22-reverse primer: TCCGCCAGGTTACTCAACAC

Graphical abstract

The graphical abstract was partially created using icons (as is, or modified) from BioRender. Ramakrishna, N. (2025) https://BioRender.com/h26g880. Other original icons were made on Adobe Illustrator.

Supplemental References

1. Clark, M.M., Hildreth, A., Batalov, S., Ding, Y., Chowdhury, S., Watkins, K., Ellsworth, K., Camp, B., Kint, C.I., Yacoubian, C., et al. (2019). Diagnosis of genetic diseases in seriously ill children by rapid whole-genome sequencing and automated phenotyping and interpretation. Sci. Transl. Med. 11. https://doi.org/10.1126/scitranslmed.aat6177.

2. Traspas, R.M., Teoh, T.S., Wong, P.-M., Maier, M., Chia, C.Y., Lay, K., Ali, N.A., Larson, A., Mutairi, F.A., Al-Sannaa, N.A., et al. (2022). Loss of FOCAD, operating via the SKI messenger RNA surveillance pathway, causes a pediatric syndrome with liver cirrhosis. Nat. Genet. 54, 1214–1226. https://doi.org/10.1038/s41588-022-01120-0.

3. Trujillano, D., Bertoli-Avella, A.M., Kandaswamy, K.K., Weiss, M.E., Köster, J., Marais, A., Paknia, O., Schröder, R., Garcia-Aznar, J.M., Werber, M., et al. (2017). Clinical exome sequencing: results from 2819 samples reflecting 1000 families. Eur. J. Hum. Genet. 25, 176–182. https://doi.org/10.1038/ejhg.2016.146.

4. Schwarz, J.M., Rödelsperger, C., Schuelke, M., and Seelow, D. (2010). MutationTaster evaluates disease-causing potential of sequence alterations. Nat. Methods 7, 575–576. https://doi.org/10.1038/nmeth0810-575.

5. Tayoun, A.A., Sinha, S., Rabea, F., Ramaswamy, S., Chekroun, I., Naofal, M.E., Jain, R., Alfalasi, R., Halabi, N., Yaslam, S., et al. (2024). Long read sequencing enhances pathogenic and novel variation discovery in patients with rare diseases. Research Square. https://doi.org/10.21203/rs.3.rs-4235049/v1.

6. Aref-Eshghi, E., Kerkhof, J., Pedro, V.P., France, G.D., Barat-Houari, M., Ruiz-Pallares, N., Andrau, J.-C., Lacombe, D., Van-Gils, J., Fergelot, P., et al. (2020). Evaluation of DNA Methylation Episignatures for Diagnosis and Phenotype Correlations in 42 Mendelian Neurodevelopmental Disorders. Am J Hum Genetics 106, 356–370. https://doi.org/10.1016/j.ajhg.2020.01.019.

7. Levy, M.A., McConkey, H., Kerkhof, J., Barat-Houari, M., Bargiacchi, S., Biamino, E., Bralo, M.P., Cappuccio, G., Ciolfi, A., Clarke, A., et al. (2022). Novel diagnostic DNA methylation episignatures expand and refine the epigenetic landscapes of Mendelian disorders. Hum. Genet. Genom. Adv. 3, 100075. https://doi.org/10.1016/j.xhgg.2021.100075.

8. Li, H. (2018). Minimap2: pairwise alignment for nucleotide sequences. Bioinformatics 34, 3094–3100. https://doi.org/10.1093/bioinformatics/bty191.

9. Bergström, A., McCarthy, S.A., Hui, R., Almarri, M.A., Ayub, Q., Danecek, P., Chen, Y., Felkel, S., Hallast, P., Kamm, J., et al. (2020). Insights into human genetic variation and population history from 929 diverse genomes. Science 367. https://doi.org/10.1126/science.aay5012.

10. Almarri, M.A., Haber, M., Lootah, R.A., Hallast, P., Turki, S.A., Martin, H.C., Xue, Y., and Tyler-Smith, C. (2021). The genomic history of the Middle East. Cell 184, 4612-4625.e14. https://doi.org/10.1016/j.cell.2021.07.013.

11. Martiniano, R., Haber, M., Almarri, M.A., Mattiangeli, V., Kuijpers, M.C.M., Chamel, B., Breslin, E.M., Littleton, J., Almahari, S., Aloraifi, F., et al. (2024). Ancient genomes illuminate Eastern Arabian population history and adaptation against malaria. Cell Genom. 4, 100507. https://doi.org/10.1016/j.xgen.2024.100507.

12. Browning, S.R., and Browning, B.L. (2007). Rapid and Accurate Haplotype Phasing and Missing-Data Inference for Whole-Genome Association Studies By Use of Localized Haplotype Clustering. Am. J. Hum. Genet. 81, 1084–1097. https://doi.org/10.1086/521987.

13. Browning, B.L., Tian, X., Zhou, Y., and Browning, S.R. (2021). Fast two-stage phasing of large-scale sequence data. Am. J. Hum. Genet. 108, 1880–1890. https://doi.org/10.1016/j.ajhg.2021.08.005.

14. Browning, S.R., Waples, R.K., and Browning, B.L. (2023). Fast, accurate local ancestry inference with FLARE. Am. J. Hum. Genet. 110, 326–335. https://doi.org/10.1016/j.ajhg.2022.12.010.

15. Gouy, M., Tannier, E., Comte, N., and Parsons, D.P. (2020). Multiple Sequence Alignment, Methods and Protocols. Methods Mol. Biol. (Clifton, NJ) 2231, 241–260. https://doi.org/10.1007/978-1-0716-1036-7_15.

16. Cetinkaya, A., Xiong, J.R., Vargel, İ., Kösemehmetoğlu, K., Canter, H.İ., Gerdan, Ö.F., Longo, N., Alzahrani, A., Camps, M.P., Taskiran, E.Z., et al. (2016). Loss-of-Function Mutations in ELMO2 Cause Intraosseous Vascular Malformation by Impeding RAC1 Signaling. Am. J. Hum. Genet. 99, 299–317. https://doi.org/10.1016/j.ajhg.2016.06.008.

17. Vangipuram, M., Ting, D., Kim, S., Diaz, R., and Schüle, B. (2013). Skin Punch Biopsy Explant Culture for Derivation of Primary Human Fibroblasts. J. Vis. Exp., e3779. https://doi.org/10.3791/3779.

18. Woods, H., Schiano, D.L., Aguirre, J.I., Ledwitch, K.V., McDonald, E.F., Voehler, M., Meiler, J., and Schoeder, C.T. (2023). Computational modeling and prediction of deletion mutants. Structure *31*, 713-723.e3. https://doi.org/10.1016/j.str.2023.04.005.

19. Abramson, J., Adler, J., Dunger, J., Evans, R., Green, T., Pritzel, A., Ronneberger, O., Willmore, L., Ballard, A.J., Bambrick, J., et al. (2024). Accurate structure prediction of

biomolecular interactions with AlphaFold 3. Nature, 1–3. https://doi.org/10.1038/s41586-024-07487-w.